Ozone Reactions with Alkaline-Earth Metal Cations and Dications in the Gas Phase: Room-Temperature Kinetics and Catalysis

S. Feil,[†] G. K. Koyanagi,[†] A. A. Viggiano,[‡] and D. K. Bohme*,[†]

Department of Chemistry, Centre for Research in Mass Spectrometry and Centre for Research in Earth and Space Science, York University, Toronto, Ontario, Canada M3J 1P3, and Air Force Research Laboratory, Space Vehicles Directorate, 29 Randolph Road, Hanscom Air Force Base, Massachusetts 01731-3010

Received: August 27, 2007; In Final Form: October 15, 2007

Room-temperature rate coefficients and product distributions are reported for the reactions of ozone with the cations and dications of the alkaline-earth metals Ca, Sr, and Ba. The measurements were performed with a selected-ion flow tube (SIFT) tandem mass spectrometer in conjunction with either an electrospray (ESI) or an inductively coupled plasma (ICP) ionization source. All the singly charged species react with ozone by O-atom transfer and form monoxide cations rapidly, $k = 4.8$, 6.7, and 8.7×10^{-10} cm^3 molecule^{-1} s^{-1} for the reactions of Ca^+, Sr^+, and Ba^+, respectively. Further sequential O-atom transfer occurs to form dioxide and trioxide cations. The efficiencies for all O-atom transfer reactions are greater than 10%. The data also signify the catalytic conversion of ozone to oxygen with the alkaline-earth metal and metal oxide cations serving as catalysts. Ca^{2+} reacts rapidly with O_3 by charge separation to form CaO^+ and O_2^+ with a rate coefficient of $k = 1.5 \times 10^{-9}$ cm^3 molecule^{-1} s^{-1}. In contrast, the reactions of Sr^{2+} and Ba^{2+} are found to be slow and add O_3, ($k \geq 1.1 \times 10^{-11}$ cm^3 molecule^{-1} s^{-1}). The initial additions are followed by the rapid sequential addition of up to five O_3 molecules with values of k between 1 and 5×10^{-10} cm^3 molecule^{-1} s^{-1}. Metal/ozone cluster ions as large as $Sr^{2+}(O_3)_5$ and $Ba^{2+}(O_3)_4$ were observed for the first time.

1. Introduction

The first study of reactions of alkaline-earth metal cations with ozone was reported in 1968 when it was found that Mg^+ and Ca^+ react rapidly to form oxide cations with rate coefficients of the order of 2×10^{-10} cm^3 molecules^{-1} s^{-1}.[1] More complicated ions also were formed in sequential chemistry, including the di- and trioxide cations, as well as oxide ions containing two and three metal atoms.[1] Since that time, the rate coefficient for the Mg^+ reaction was remeasured and a value 3 times higher was found.[2] These ions were chosen for study in part because of the application to the earth's ionosphere where they can appear as a consequence of the ablation of interplanetary dust particles.[1−4] Very recently the group of Plane has reported kinetic results for reactions between Ca^+ ($4^2S_{1/2}$) and O_3, O_2, N_2, CO_2, and H_2O.[5] These reactions were studied using two techniques: the pulsed laser photodissociation at 193 nm of an organo−calcium vapor, followed by time-resolved laser-induced fluorescence spectroscopy of Ca^+ at 393.37 nm ($Ca^+(4^2P_{3/2}–4^2S_{1/2})$), and the pulsed laser ablation at 532 nm of a calcite target in a fast flow tube, followed by mass spectrometric detection of Ca^+. The rate coefficient for the reaction with O_3 was found to be essentially independent of temperature between 189 and 312 K with a value of $(3.9 \pm 1.2) \times 10^{-10}$ cm^3 molecule^{-1} s^{-1}.

An inductively coupled plasma (ICP) recently was employed as a source for atomic metal ions in conjunction with a selected-ion flow tube (SIFT) apparatus at York University.[6] This combination has proven to provide a powerful tool for studies of chemical reactions with atomic cations including the heavier alkaline-earth metal cations Ca^+, Sr^+, and Ba^+.[7−9] Also, a triple-quadrupole mass spectrometer (with extended mass range) now has been added after the flow tube, and this configuration, symbolized as ICP/qQ/SIFT/QqQ (q represents a focusing only quadrupole and Q a mass-selective one), provides even more versatility in such studies. The latest change of the experimental setup was to interface an electrospray ionization (ESI) source with the SIFT apparatus.[10] This most recent experimental configuration, symbolized as ESI/qQ/SIFT/QqQ, was designed primarily for the investigation of biological cations and anions, but it also allows studies of reactions with atomic cations and dications. Both combinations have been employed in the present work in the measurement of rates and product distributions for reactions of ozone with the cations and dications of Ca, Sr, and Ba, and the two means of cation formation (ICP and ESI) are compared with each other. Ozone can be expected to oxidize all these cations since it has a particularly low O_2−O bond strength. Reactions of ozone with dications appear not to have been reported previously.

This paper represents the first in a series of studies of ozone reactions that exploit the unique SIFT capabilities of the York University laboratory in combination with the considerable experience of the Air Force Research Laboratory (AFRL) group with ozone chemistry. The latter has shown that only reactions for which the O_3 rate coefficient is roughly 20 times larger than that for O_2 can be easily studied, since the O_3 is generated as a dilute mixture in O_2 (3−5%).[11−15] Since O_2 is rarely reactive,[8,16,17] this is usually not a serious constraint.

2. Experimental Section

The experiments were performed with a multisource, multisector selected-ion flow tube tandem mass spectrometer,

* Corresponding author. E-mail: dkbohme@yorku.ca.
[†] York University.
[‡] Air Force Research Laboratory.

10.1021/jp076855g CCC: $37.00
Published on Web 12/01/2007

symbolized as ESI(ICP)/qQ/SIFT/QqQ, developed in the Ion Chemistry Laboratory at York University. The atomic ions were generated either in an ICP[6] or an ESI[10] source with a microspray emitter needle.

Cations and dications of Ca, Sr, and Ba were generated with ESI from 30 μM solutions of calcium acetate in 100% methanol, strontium acetate in water/methanol (80/20), and barium chloride in water/methanol (80/20). For the generation of atomic cations in the ICP, solutions containing the metal salt of interest with concentration of approximately 5 μg L^{-1} were peristaltically pumped via a nebulizer into the plasma. The preparation of the solutions has been described previously.[7] The alkali earth cations emerge from the ICP in a large excess of Ar^+.

The bare cations and dications emerging from the ICP or the ESI source are mass selected and injected through a Venturi-type aspirator into the flow tube that is flushed with helium at 0.35 ± 0.01 Torr. Before reaching the reaction region, the ions undergo multiple collisions with helium ($\sim 4 \times 10^5$) to ensure translational thermalization. The large number of collisions with the helium buffer gas atoms ensures that the atomic ions reach a translational temperature equal to the tube temperature of 292 $\pm$ 2 K prior to entering the reaction region. The ions are allowed to react with added neutral gas in the reaction region, and then they are sampled along with product ions and analyzed in a triple-quadrupole mass spectrometer. The reactant and product ion signals are monitored as a function of the flow of the reagent gas. Primary rate coefficients are determined from the observed semilogarithmic decay of the primary reactant ion intensity using pseudo-first-order kinetics. The rate coefficients for the primary reactions reported herein have an absolute accuracy estimated to be $\pm$30%.

The ozone generator and detection system are the ones used in a number of experiments at the AFRL.[11−15] Ozone is generated by passing oxygen gas through an Orec O3V-0 ozonator. The absolute concentration of O_3 is measured by optical absorption at 248 nm using a Perkin-Elmer Lambda 10 UV−vis spectrometer. The total pressure in the absorption cell is also measured. Combining the concentration and pressure measurements shows that the percentage of O_3 was $\sim$4.5%.

3. Results and Discussion

3.1. Stoichiometry and Thermodynamics of Reactions with O_2. The alkaline-earth metal cations Ca^+, Sr^+, and Ba^+, even though they have radical (s^1) character and are isoelectronic with K, Rb, and Cs, respectively, are not expected to be very reactive, even with molecular oxygen, $O_2(X^3\Sigma)$, a diradical. The electron recombination energies of Ca^+ (IE(Ca) = 6.113 eV), Sr^+ (IE(Sr) = 5.695 eV), and Ba^+ (IE(Ba) = 5.212 eV) are too small to thermodynamically allow electron transfer from O_2, IE(O_2) = 12.0697 $\pm$ 0.0002 eV.[18] Electron transfer is endothermic by at least 5.96 eV. Furthermore, O-atom transfer from O_2 ($D(O_2)$ = 123.89 $\pm$ 0.02 kcal mol^{-1})[18] to Ca^+ (OA(Ca^+) = 77.2 kcal mol^{-1}), Sr^+ (OA(Sr^+) = 71.4 kcal mol^{-1}), and Ba^+ (OA(Ba^+) = 92.8 kcal mol^{-1})[19] is endothermic by at least 31 kcal mol^{-1}. So the observation of these bimolecular ion−molecule reactions of Ca^+, Sr^+, and Ba^+ with O_2 is not expected. Indeed, only the slow, presumably termolecular, addition of O_2 to form dioxide cations was observed with effective bimolecular rate coefficients $k \geq$ 6.8, 2.0, and 3.4×10^{-13} cm^3 $molecule^{-1}$ s^{-1} for Ca^+, Sr^+, and Ba^+, respectively.

The doubly charged ions Ca^{2+}, Sr^{2+}, and Ba^{2+} are isolectronic with Ar, Kr, and Xe, respectively, and so have a rare-gas electronic configuration. Bimolecular reaction channels that are stoichiometrically possible for reactions of these dications with molecular oxygen are indicated in reaction 1.

$$M^{2+} + O_2 \rightarrow MO^{2+} + O \quad (1a)$$

$$\rightarrow MO^+ + O^+ \quad (1b)$$

$$\rightarrow MO + O^{2+} \quad (1c)$$

$$\rightarrow M^+ + O_2^+ \quad (1d)$$

$$\rightarrow M + O_2^{2+} \quad (1e)$$

$$\rightarrow M + O^+ + O^+ \quad (1f)$$

The thermodynamics for the oxidation of the doubly charged ions Ca^{2+}, Sr^{2+}, and Ba^{2+} to form oxide dications MO^{2+}, reaction 1a, is not well-known but will be endothermic unless $OA(M^{2+}) > D(O_2) = 124$ kcal mol^{-1}. $IE_2(M) <$ IE(O) = 13.618 eV so that O-atom transfer with charge separation (reaction 1b) is endothermic, as is reaction 1c, which would require the double ionization of O, $IE_1(O) + IE_2(O) = 48.74$ eV. Single-electron transfer (reaction 1d) is endothermic by at least 0.20 eV (IE_2 = 11.871 (Ca), 11.030 (Sr), 10.004 eV (Ba)).[20] Two-electron transfer (reaction 1e) is probably endothermic as well: the sum of the first two ionization energies of Ca, Sr, and Ba is as high as 17.98 eV (for Ca) but almost certainly still too small to lead to the double ionization of O_2 (or the formation of two O^+ via reaction 1f). So bimolecular ion−molecule reactions of Ca^{2+}, Sr^{2+}, and Ba^{2+} with O_2 are not expected, and they were not observed. Some O_2 addition was observed with Sr^{2+} and Ba^{2+} with effective bimolecular rate coefficients of $\geq 6.5 \times 10^{-13}$ and 1.3×10^{-12} cm^3 $molecule^{-1}$ s^{-1}, respectively.

3.2. Stoichiometry and Thermodynamics of Reactions with O_3. In contrast to oxygen, observable bimolecular reactions are expected with ozone. The very weak O_2−O bond in ozone, $D(O_2-O) = 25.5 \pm 0.1$ kcal mol^{-1}, makes the oxidation of the alkaline-earth metal cations, reaction 2a, exothermic by at least 45.9 kcal mol^{-1}. Reaction 2b might be less exothermic, but $D(MO^+-O)$ appears not to be known for M = alkaline-earth metal.

$$M^+ + O_3 \rightarrow MO^+ + O_2 \quad (2a)$$

$$\rightarrow MO_2^+ + O \quad (2b)$$

$$\rightarrow M + O_3^+ \quad (2c)$$

Since $IE(O_3) = 12.53 \pm 0.08$ eV,[18] electron transfer to M^+ according to reaction 2c is endothermic by at least 6.43 eV.

Although generally not well-known for reactions of doubly charged cations with ozone, thermodynamics may well favor channel 3c among the bimolecular reactions 3a−3e. This channel is governed by $-IE(M^+) - OA(M^+) + IE(O_2) + D(O_2-O)$ and is exothermic by 2.05, 0.96, and 0.86 eV for the reactions of Ca^{2+}, Sr^{2+}, and Ba^{2+}, respectively.

$$M^{2+} + O_3 \rightarrow MO^{2+} + O_2 \quad (3a)$$

$$\rightarrow MO_2^{2+} + O \quad (3b)$$

$$\rightarrow MO^+ + O_2^+ \quad (3c)$$

$$\rightarrow MO_2^+ + O^+ \quad (3d)$$

$$\rightarrow M + O_3^{2+} \quad (3e)$$

$$\rightarrow M + O_2^+ + O^+ \quad (3f)$$

Channel 3a will be exothermic if $OA(M^{2+}) > OA(O_2) = 25.5$ kcal mol^{-1}, and this may well be so (but $OA(M^{2+})$ is not known). Intramolecular electron transfer from O_2, $IE(O_2) = 12.07$ eV, to MO^{2+} before these two products separate could then favor channel 3c if $RE(MO^{2+}) > 12.07$ eV, but it is not known. Channel 3b would be exothermic if the O_2 affinity of $M^{2+} > 25.5$ kcal mol^{-1}, but it also is not known. Intramolecular electron transfer from O, $IE(O) = 13.618$ eV, to MO_2^{2+} would lead to channel 3d if $RE(MO_2)^{2+} > 13.618$ eV, but $RE(MO_2^{2+})$ is not known. The two-electron transfer (channel 3e) would be exothermic if $IE(O_3) + IE(O_3^+) < IE(M) + IE(M^+)$, but $IE(O_3^+)$ is not known. O_3^{2+} likely would dissociate into O_2^+ and O^+, and this channel (channel 3f) is endothermic overall since $IE(O_2) + IE(O) + D(O_2{-}O) > IE(M) + IE(M^+)$.

3.3. Observed Kinetics for Reactions of M^+ with Ozone. Figure 1 shows the raw data obtained for Ca^+ and Ar^+ born in the ICP source reacting with the O_3/O_2 mixture added into the flow tube. The Ar^+ and Ca^+ ions could not be resolved with our quadrupole mass selector, but the decay of the *m*/*z* 40 peak in the left panel of Figure 1 exhibits two clearly distinguishable slopes. The early fast decay can be attributed to the reaction of Ar^+ with ozone and O_2, while the later and slower decay can be attributed solely to the reaction of Ca^+ ions with ozone. Fitting the two slopes provides rate coefficients for the decay of Ar^+ with added ozone of 1.1×10^{-9} cm^3 molecule^{-1} s^{-1} and the decay of Ca^+ of 4.9×10^{-10} cm^3 molecule^{-1} s^{-1}. The known electron-transfer reaction of Ar^+ with the O_2 that accompanies the addition of ozone (in a ratio of 22.2:1) has a rate coefficient[16] of ca. 4×10^{-11} cm^3 molecule^{-1} s^{-1} which, by pure coincidence, is about 20 times slower than the faster reaction with ozone, and so leads to an indistinguishable decay in the Ar^+ ion signal under our operating conditions.

The decline in the Ca^+ ion signal in Figure 1 is accompanied by the sequential production of CaO^+, CaO_2^+, CaO_3^+, and CaO_6^+ that can be attributed to reactions 4−7.

$$Ca^+ + O_3 \rightarrow CaO^+ + O_2 \quad (4)$$

$$CaO^+ + O_3 \rightarrow CaO_2^+ + O_2 \quad (5)$$

$$CaO_2^+ + O_3 \rightarrow CaO_3^+ + O_2 \quad (6)$$

$$CaO_3^+ + O_3 + He/O_2 \rightarrow CaO_3(O_3)^+ + He/O_2 \quad (7)$$

The observed rise in O_2^+ in Figure 1 is due to the known electron transfer from O_2 to Ar^+ (electron transfer from O_2 to Ca^+ is endothermic), perhaps also due to a dissociative electron transfer from O_3, and indirectly from the electron-transfer reaction with O_3, since O_3^+ is known to react with O_2 by electron transfer with $k = 2.9 \times 10^{-10}$ cm^3 molecule^{-1} s^{-1}.[21] The production of O_3^+ is attributed to the reaction of ozone with Ar^+ alone (electron transfer from O_3 to Ca^+ is endothermic).

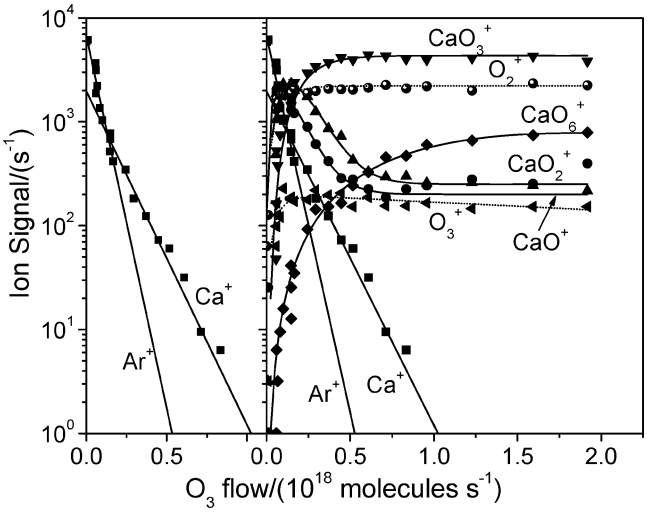

Figure 1. Ion signals recorded for the reaction of selected *m*/*z* 40 cations with a 4.5% mixture of O_3 in O_2. The left panel shows a fit to the decay of the *m*/*z* 40 cation assigned to a fast reaction of Ar^+ and a slower reaction of Ca^+. The right panel includes the profiles measured for the observed product ions. Not shown for clarity are the ions $CaO_{1,2,3}(H_2O)^+$ that arise from water impurity in the flowing helium.

TABLE 1: Rate Coefficients (in Units of cm^3 molecule^{-1} s^{-1}), Reaction Efficiencies, Ion Products, and Reaction Enthalpies for the Reactions of Alkaline-Earth Metal Cations and Dications with O_3

ion	k (ESI)[a]	k (ICP)[a]	k_{coll}[b]	ion products	$-\Delta H°_{298}$[c]
Ca^+	4.7×10^{-10}	4.9×10^{-10}	1.1×10^{-9}	CaO^+	−52
Sr^+	6.5×10^{-10}	6.9×10^{-10}	9.0×10^{-10}	SrO^+	−46
Ba^+	8.6×10^{-10}	8.8×10^{-10}	8.4×10^{-10}	BaO^+	−68
Ca^{2+}	1.5×10^{-9}		2.1×10^{-9}	$CaO^+;O_2^+$	−48
Sr^{2+}	$\geq 3.2 \times 10^{-11}$		1.8×10^{-9}	SrO_3^{2+}	
Ba^{2+}	$\geq 1.1 \times 10^{-11}$		1.7×10^{-9}	BaO_3^{2+}	
CaO^+	$\geq 5.7 \times 10^{-10}$	$\geq 1.2 \times 10^{-9}$	9.9×10^{-10}	CaO_2^+	
CaO_2^+	$\geq 1.4 \times 10^{-9}$	$\geq 1.2 \times 10^{-9}$	9.4×10^{-10}	CaO_3^+	
SrO^+	$\geq 5.2 \times 10^{-10}$	$\geq 3.5 \times 10^{-10}$	8.8×10^{-10}	SrO_2^+	
SrO_2^+	$\geq 8.8 \times 10^{-10}$	$\geq 8.2 \times 10^{-10}$	8.6×10^{-10}	SrO_3^+	
BaO^+	$\geq 2.1 \times 10^{-10}$	$\geq 1.5 \times 10^{-10}$	8.3×10^{-10}	BaO_2^+	
BaO_2^+	$\geq 1.0 \times 10^{-9}$	$\geq 7.9 \times 10^{-10}$	8.2×10^{-10}	BaO_3^+	

[a] Effective bimolecular reaction rate coefficient measured in helium at 0.35 Torr and 293 K. The uncertainties are estimated to be 30% for the primary reactions and 50% for the higher-order reactions. Ions were generated either by electrospray ionization (ESI) or in an inductively coupled plasma (ICP). [b] k_{coll} is the capture or collision rate coefficient computed using the algorithm of the modified variational transition-state/classical trajectory theory developed by Su and Chesnavich (ref 22) with a polarizability, $\alpha(O_3) = 3.12$ Å^3 (ref 23) and dipole moment, $\mu_D = 0.534$ D (ref 23). [c] Reaction enthalpy in kcal mol^{-1} derived from ref 18.

The lines are model fits to the data. The rate coefficients used in the modeling are listed in Table 1, along with collision rate coefficients and reaction enthalpies. The modeling assumes that reactions with O_2 are negligible for all reactants. The reaction of Ca^+ with O_2 was studied separately and was observed to proceed very slowly by O_2 addition, $k \geq 6.8 \times 10^{-13}$ cm^3 molecule^{-1} s^{-1}. Since the O_3 rate coefficient is 720 times larger and the concentration ratio is 22.2, the assumption seems justified in this case. Measurements of the reactions of the oxide cations with O_2 were not possible, but these cations are also expected to react by slow addition; oxidation is expected to be endothermic because of the strength of the O_2 bond.

The alkaline-earth metal monocations also could be generated using ESI. This is useful for the study of reactions of Ca^+ since the isobaric interference with Ar^+ is absent. Figure 2 presents a comparison of the data obtained with the two modes of

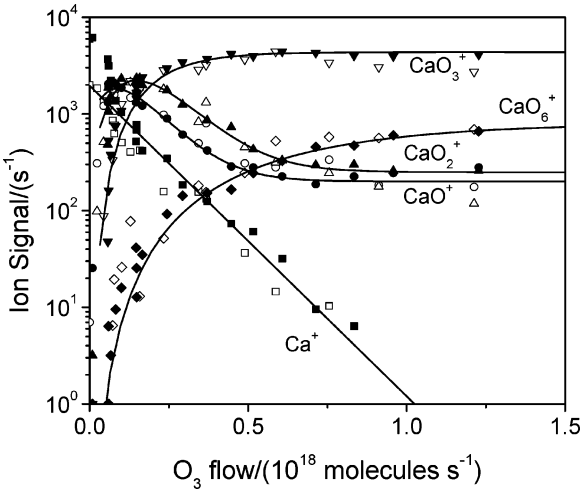

Figure 2. Ion signals recorded for the reaction of the selected *m*/*z* 40 cation derived from an ICP (solid points) and by ESI (open points) with a 4.5% mixture of O_2 and O_3. Not shown for clarity are the ions $CaO_{1,2,3}(H_2O)^+$ that arise by addition of water impurity in the flowing helium.

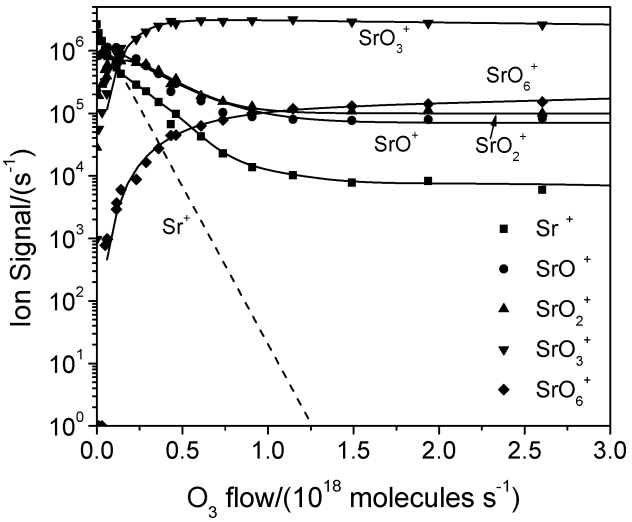

Figure 3. Ion signals recorded for the reaction of selected Sr^+ cations derived by ESI with an added 4.5% mixture of O_2 and O_3.

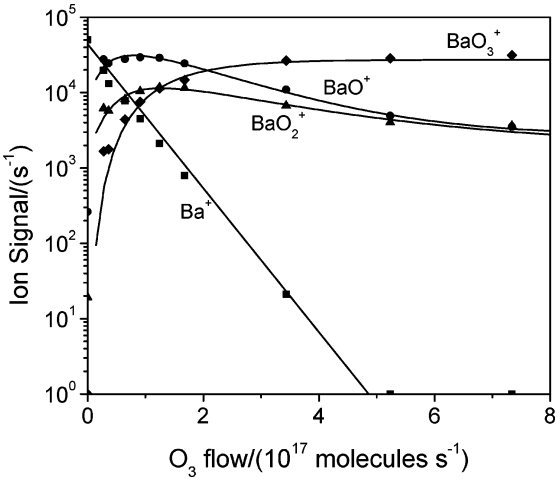

Figure 4. Ion signals recorded for the reaction of the selected Ba^+ cations derived by ESI with an added 4.5% mixture of O_2 and O_3.

ionization (ESI and ICP) for Ca^+ reacting with ozone. There is excellent agreement in the observed ion profiles between the two means of ion formation.

All three of the singly charged alkaline-earth metal cations were studied with both ion sources, and this comparison illustrates another important point. The uncertainty associated with the unknown relative population of excited and ground electronic states in the reaction region that arises when the ICP is used as a source disappears when these cations are produced in the electrosprayed solution in which excited electronic states presumably are absent. The excited-state percentages estimated for Ca^+, Sr^+, and Ba^+ *within the ICP* are 12.5%, 10.0%, and 55.6%, respectively.[8] Therefore the agreement observed for the reactions of these three ions, especially Ba^+, produced in the ICP or by ESI (see Table 1) suggests either the occurrence of excited-state relaxation in the ICP experiments or an independence of the measured rate coefficient on the extent of electronic excitation. Rate coefficients derived for the higher-order oxidation reactions determined in these two different ways also are included in Table 1, and there is generally agreement within the experimental uncertainties.

The reaction of Ca^+ with O_3 has been previously studied with a flowing afterglow apparatus.[1] The rate coefficient was found to be only 1.6×10^{-10} cm^3 molecule^{-1} s^{-1} which is about 3 times lower than our values of 4.7 (ESI) and 4.9 (ICP) $\times 10^{-10}$ cm^3 molecule^{-1} s^{-1}. The Ca^+ was derived by electron impact ionization of Ca vapor in the earlier measurements. Since the electron-transfer reaction of CaO^+ with Ca is exothermic, the occurrence of this reaction with the Ca vapor flowing down the tube would lead to the production of Ca^+ and so an artificially small rate constant for the Ca^+ reaction with O_3. The concomitant observation of species with multiple calcium atoms, namely, $Ca_2O_2^+$, $Ca_2O_3^+$, and $Ca_2O_4^+$, also indicates that enough Ca was present to be ionized by CaO^+. No such interference is possible in the present experiments. Our results are in much better agreement, within experimental error, with the very recent measurements reported by Broadley et al.[5] The temperature-independent value of $(3.9 \pm 1.2) \times 10^{-10}$ cm^3 molecule^{-1} s^{-1} reported by that group agrees, within experimental error, with our average value of $(4.8 \pm 1.4) \times 10^{-10}$ cm^3 molecule^{-1} s^{-1}.

The results of our measurements for Sr^+ and Ba^+ reacting with O_3 are quite similar to those for Ca^+. Apparently no previous measurements have been made for either system. Both ions react with O_3 by O-atom transfer with close to unit efficiency to produce SrO^+ and BaO^+, respectively. These two oxides also react further by O-atom transfer to form dioxide and trioxide cations (see Figures 3 and 4).

Table 1 shows that there is a trend in the rate and efficiency of the O-atom transfer reaction 2a: both increase as one moves down the periodic table. The average values of the ICP and ESI rate coefficient measurements are 4.8, 6.7, and 8.7 $\times 10^{-10}$ cm^3 molecule^{-1} s^{-1}, and the efficiencies (k/k_c) based on these values are 0.44, 0.73, and 1.0, for the reactions with Ca^+, Sr^+, and Ba^+, respectively (see Table 1). These trends do *not* follow the trend in exothermicity based on known values for the O-atom affinities of the three alkaline-earth metal cations (see Table 1). The exothermicity of the reaction with Sr^+ for which OA is reported to be 71.4 kcal mol^{-1} does not fall between the exothermicities of the reactions with Ca^+ and Ba^+ which are reported as 77.2 and 92.8 kcal mol^{-1}, respectively. However the reaction with Ba^+, which exhibits unit efficiency, is by far the most exothermic.

3.4. Catalytic Conversion of Ozone to Oxygen. It is noteworthy from Figures 1−4 that the kinetic profiles of the lower oxide cations as well as Sr^+ are curved. These curvatures can be attributed to the occurrence of reactions of type 8−10 which will be exothermic if OA(M^+), OA(MO^+), and OA-

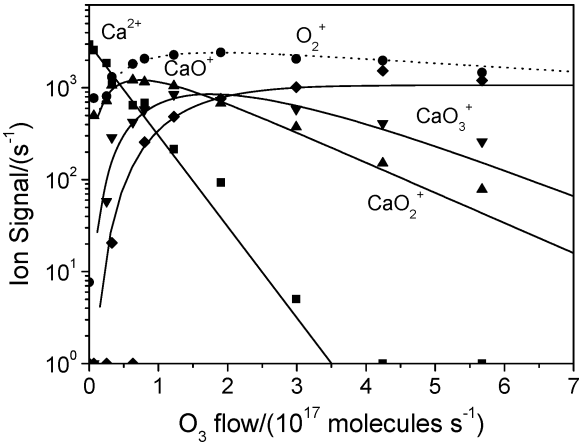

Figure 5. Ion signals recorded for the reaction of the selected Ca^{2+} produced by ESI with an added 4.5% mixture of O_2 and O_3.

SCHEME 1: Catalytic Cycle for the Cation-Catalyzed Conversion of Ozone to Oxygen[a]

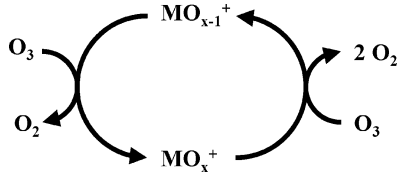

[a] Here M is an alkaline-earth metal.

$(MO_2^+) < D(O-O) - D(O_2-O)$ or <98.5 kcal mol^{-1}. This is known to be the case

$$MO^+ + O_3 \rightarrow M^+ + 2O_2 \quad (8)$$

$$MO_2^+ + O_3 \rightarrow MO^+ + 2O_2 \quad (9)$$

$$MO_3^+ + O_3 \rightarrow MO_2^+ + 2O_2 \quad (10)$$

for reactions of type 8 since $OA(Ca^+) = 77.2$ kcal mol^{-1}, $OA(Sr^+) = 71.4$ kcal mol^{-1}, and $OA(Ba^+) = 92.8$ kcal mol^{-1}.[20] Indeed, Rowe et al.[2] reported many years ago the occurrence at 300 K of reaction 8 for MgO^+ with $k = 8 \times 10^{-10}$ cm^3 molecule^{-1} s^{-1}. The oxygen atom affinities of the MO^+ and MO_2^+ cations are less certain.

Reactions 8−10 together with reaction 2a and analogous reactions with the metal oxides constitute the catalytic cycle shown in Scheme 1 in which ozone is converted to oxygen according to reaction 11 which is exothermic by 68 kcal mol^{-1}.[18]

$$2O_3 \rightarrow 3O_2 \quad (11)$$

We are confident that the occurrence of this catalytic cycle within the reaction region of the flow tube is responsible for the curvatures that were observed in the ion signal profiles. The occurrence of the back-reactions of type 12 can be ruled out even in the presence of the added oxygen since they are (see Table 1), or are expected to be, too endothermic.

$$MO_x^+ + O_2 \rightarrow MO_{x-1}^+ + O_3 \quad (12)$$

3.5. Observed Kinetics for Reactions of M^{2+} with Ozone. The reactions of the doubly charged alkaline-earth metal ions with ozone proved to be very interesting. Only Ca^{2+} (Figure 5) was found to react rapidly with O_3. The reaction proceeds at 70% of the collision value (see Table 1) by O^- transfer and charge separation to produce CaO^+ and O_2^+ according to reaction 13.

$$Ca^{2+} + O_3 \rightarrow CaO^+ + O_2^+ \quad (13)$$

Single-electron transfer is endothermic since the ionization energy of O_3 is greater than the second-ionization energy of Ca, but formation of $CaO^+ + O_2^+$ is exothermic by about 2.05 eV. Once formed, CaO^+ reacts by sequential O-atom transfer in the manner shown in eqs 5 and 6 and Figure 1.

The reactions of Sr^{2+} and Ba^{2+} with ozone behaved much differently than that with Ca^{2+}; no charge separation was observed with Sr^{2+} and Ba^{2+}, even though it is exothermic by more than 0.8 eV with both dications. Ozone addition was observed instead, presumably according to the termolecular reactions 14 and 15, as is evident in Figures 6 and 7.

$$Sr^{2+}(O_3)_n + O_3 + He/O_2 \rightarrow Sr^{2+}(O_3)_{n+1} + He/O_2 \quad n = 1-5 \quad (14)$$

$$Ba^{2+}(O_3)_n + O_3 + He/O_2 \rightarrow Ba^{2+}(O_3)_{n+1} + He/O_2 \quad n = 1-4 \quad (15)$$

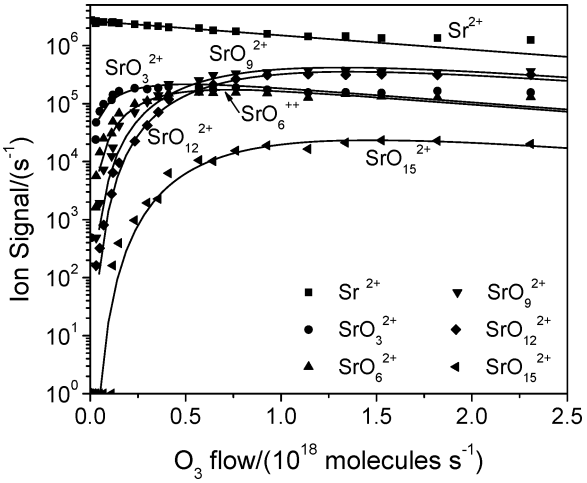

Figure 6. Ion signals recorded for the reaction of the selected Sr^{2+} produced by ESI with an added 4.5% mixture of O_2 and O_3. $Sr(H_2O)_n^{2+}$ for $n = 1-4$; $SrO_3nH_2O^{2+}$ for $n = 1-4$; $SrO_3(H_2O)_2^{2+}$ and $SrO_6(H_2O)_2^{2+}$ clusters also were observed but are omitted in the figure for clarity.

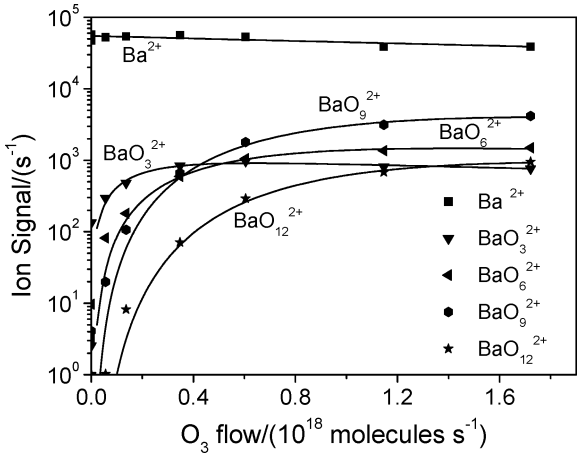

Figure 7. Ion signals recorded for the reaction of the selected Ba^{2+} produced by ESI with an added 4.5% mixture of O_2 and O_3. $Ba^{2+}(H_2O)_{1,2}$, $Ba^{2+}(H_2O)(O_3)_{1,2}$ were observed as well but omitted for more clarity.

The fits to the reaction profiles shown in Figures 6 and 7 provide effective bimolecular rate coefficients for all these addition reactions with quite high values between 1 and 5×10^{-10} cm^3 molecule^{-1} s^{-1}. The observation of metal/ozone cluster ions as large as $Sr^{2+}(O_3)_5$ and $Ba^{2+}(O_3)_4$ is fascinating and should stimulate theoretical and experimental studies directed at an elucidation of their structures.

It is interesting to speculate why only the Ca^{2+} reacts by charge separation. Doubly charged ion reactions often proceed by single-electron transfer. In those cases, the magnitude of the electron-transfer rate coefficient is governed by the distance at which the ion-induced dipole attractive potential crosses the ion−ion repulsive potential.[24] Electron transfer is expected to occur when the crossing lies between 2 and 8 Å and with near unit efficiency if the crossing is at approximately 4 Å.[24] These same two curves operate in the doubly charged ion reactions investigated here, but the situation is more complicated since an O atom is also transferred. The two curves cross at 7.1, 14.5, and 15.5 Å for Ca^{2+}, Sr^{2+}, and Ba^{2+}, respectively. Thus, the crossing in the reaction with Ca^{2+} is in the window and those for the other reactions are not. More detailed calculations are needed to fully address this issue, but the simple analysis is suggestive that electrostatics play a major role. The failure of charge separation to occur at room temperature in the reactions of Sr^{2+} and Ba^{2+} with ozone also may be attributed to a Coulomb repulsion between the product ions that introduces an activation energy above the initial energy of these reactants.[25,26] The larger exothermicity in the Ca^{2+} reaction lowers the barrier enough so that the reaction occurs. It is this barrier that leads to one side of the window described above.

4. Conclusions

The alkaline-earth metal cations Ca^+, Sr^+, and Ba^+ that have been investigated all exhibit a high tendency to abstract an oxygen atom from ozone, and the efficiency of O-atom transfer increases down the periodic table. In all cases, subsequent sequential O-atom transfer leads to the formation of the dioxide and ultimately the trioxide cation that then begins to add ozone. The recorded ion profiles also point to the ability of Ca^+, Sr^+, and Ba^+ and their monoxides and dioxides to catalyze the conversion of ozone to oxygen.

An interesting transition in reactivity occurs between Ca^{2+} and Sr^{2+} for the exothermic reactions of the doubly charged alkaline-earth metal cations with ozone moving down the column on the periodic table, and charge separation with O-atom transfer becomes less exothermic. Ca^{2+} exhibits a rapid charge separation reaction, but Sr^{2+} and Ba^{2+} simply add ozone. Apparently Coulomb repulsion between the product ions in these exothermic reactions introduces an activation energy above the initial energy of these reactants.

The large extent of sequential clustering with ozone observed in the room-temperature reactions with Sr^{2+} and Ba^{2+} is somewhat unexpected, and the energetics and structures of these clusters of closed-shell dications with singlet diradical ligands certainly are of interest.

A comparative study involving production of Ca^+, Sr^+, and Ba^+ by either ESI or ICP ionization shows agreement in the rate measurements. The use of ESI has an inherent advantage since it avoids the production of electronic excited states and here has shown that the excited states of Ca^+, Sr^+, and Ba^+ produced in the ICP source are either quenched or react at the same rate as their ground states.

Acknowledgment. Continued financial support from the Natural Sciences and Engineering Research Council of Canada is greatly appreciated. Also, we acknowledge support from the National Research Council, the Natural Science and Engineering Research Council, and MDS SCIEX in the form of a Research Partnership Grant. As holder of a Canada Research Chair in Physical Chemistry, Diethard K. Bohme thanks the contributions of the Canada Research Chair Program to this research. The AFRL portion of this work was supported by the United States Air Force Office of Scientific Research (AFOSR) under Project No. 2303EP4.

References and Notes

(1) Ferguson, E. E.; Fehsenfeld, F. C. *J. Geophys. Res.* **1968**, *73*, 6215.
(2) Rowe, B. R.; Fahey, D. W.; Ferguson, E. E.; Fehsenfeld, F. C. *J. Chem. Phys.* **1981**, *75*, 3325.
(3) Plane, J. M. C. *Chem. Rev.* **2003**, *103*, 4963.
(4) Ferguson, E. E.; Rowe, B. R.; Fahey, D. W.; Fehsenfeld, F. C. *Planet. Space Sci.* **1981**, *29*, 479.
(5) Broadley, S. L.; Vondrak, T.; Plane, J. M. C. *Phys. Chem. Chem. Phys.* **2007**, *9*, 4357.
(6) Koyanagi, G. K.; Lavrov, V. V.; Baranov, V.; Bandura, D.; Tanner, S.; McLaren, J. W.; Bohme, D. K. *Int. J. Mass Spectrom.* **2000**, *194*, L1.
(7) Lavrov, V. V.; Blagojevic, V.; Koyanagi, G. K.; Orlova, G.; Bohme, D: K. *J. Phys. Chem. A* **2004**, *108*, 5610.
(8) Koyanagi, G. K.; Caraiman, D.; Blagojevic, V.; Bohme, D. K. *J. Phys. Chem. A* **2002**, *106*, 4581.
(9) Koyanagi, G. K.; Bohme, D. K. *J. Phys. Chem. A* **2006**, *110*, 1232.
(10) Koyanagi, G. K.; Baranov, V. I.; Tanner, S. D.; Anichina, J.; Jarvis, M. J. Y.; Feil, S.; Bohme, D. K. *Int. J. Mass Spectrom.* **2007**, *265*, 295.
(11) Van Doren, J. M.; Williams, S.; Midey, A. J.; Miller, T. M.; Viggiano, A. A. *Int. J. Mass Spectrom.* **2005**, *241*, 185.
(12) Viggiano, A. A.; Arnold, S. T.; Williams, S.; Miller, T. M. *Plasma Chem. Plasma Process.* **2002**, *22*, 285.
(13) Williams, S.; Campos, M. F.; Midey, A. J.; Arnold, S. T.; Morris, R. A.; Viggiano, A. A. *J. Phys. Chem. A* **2002**, *106*, 997.
(14) Fernandez, A. I.; Midey, A. J.; Miller, T. M.; Viggiano, A. A. *J. Phys. Chem. A* **2004**, *108*, 9120.
(15) Williams, S.; Knighton, W. B.; Midey, A. J.; Viggiano, A. A.; Irle, S.; Morokuma, K. *J. Phys. Chem. A* **2004**, *108*, 1980.
(16) Ikezoe, Y.; Matsuoka, S.; Takebe, M.; Viggiano, A. A. *Gas Phase Ion−Molecule Reaction Rate Constants Through 1986*; Maruzen Company, Ltd.: Tokyo, 1987.
(17) Anicich, V. *An Index of the Literature for Bimolecular Gas Phase Cation−Molecule Reaction Kinetics*; JPL Publication 03-19; NASA Jet Propulsion Laboratory, California Institute of Technology: Pasadena, CA, 2003.
(18) NIST data base. http://webbook.nist.gov/chemistry, accessed July 2007.
(19) Schröder, D.; Schwarz, H.; Shaik, S. *Structure and Bonding*; Springer-Verlag: Berlin, Heidelberg, 2000; Vol. 97, pp 91−122.
(20) Moore, C. E. *Ionization Potentials and Ionization Limits Derived from the Analyses of Optical Spectra*; NSRDS-NBS 34; U.S. National Bureau of Standards: Washington, DC, 1970.
(21) Midey, A. J.; Williams, S.; Miller, T. M.; Larsen, P. T.; Viggiano, A. A. *J. Phys. Chem. A* **2002**, *106*, 11739.
(22) Su, T.; Chesnavich, W. J. *J. Chem. Phys.* **1982**, *76*, 5183.
(23) *CRC Handbook of Chemistry and Physics*, 78th ed.; Lide, D. R., Ed.; CRC Press: Cleveland, OH, 1997−8.
(24) Dressler, R. A.; Viggiano, A. A. Charge Transfer-Fundamentals. In *Encyclopedia of Mass Spectrometry-Organic Ions*; Gross, M. L., Caprioli, R., Nibbering, N., Eds.; Elsevier: Amsterdam, 2005; Vol. 4.
(25) Petrie, S.; Javahery, G.; Wang, J.; Bohme, D. K. *J. Phys. Chem.* **1992**, *96*, 6121.
(26) Petrie, S.; Wang, J.; Bohme, D. K. *Chem. Phys. Lett.* **1993**, *204*, 473.